CRISPR/Cas9 mediated genome edition in castor plant based on Golden Gate Assembly

Villoslada Valbuena, Mónica (1), Venegas Calerón, Mónica (1), Martínez-Force, Enrique (1), Garcés, Rafael (1) and Salas Liñán, Joaquín J. (1).

(1) Department of Biochemistry and Molecular Biology of Plant Products, Instituto de la Grasa (CSIC), Sevilla, Spain

INTRODUCTION

In the last decade, CRISPR/Cas9 technology has been developed as the most efficient and widely used genome editing tool to modify plant genomes (figure 1). However, simultaneous editing of multiple targets still remains a technical challenge (Ma et al., 2014).

Among the species that accumulate unusual fatty acids, the castor bean plant (*Ricinus communis*) is particularly noteworthy. Its seeds accumulate 50-60% oil, 85-90% of which is ricinoleic acid (18:1-OH), a product from oleic acid hydroxylation catalyzed by Δ12-oleate hydroxylase (FAH12) (Shanklin et al., 1998).

OBJECTIVE

In other studies, FAH12 alteration is responsible for a decrease of the ricinoleic acid accumulation showing high oleic phenotype (Venegas-Calerón et al., 2016) or linoleic acid increase (Sánchez Álvarez, 2019). In this context, it is of great interest to continue investigating the role of this enzyme to better understand its importance in the accumulation of fatty acids.

Our main goal was obtaining an unique genetic construction through Golden Gate Assembly (Engler et al., 2014) that allows the expression of two sgRNAs together with the cas9 nuclease in the same plasmid vector to produce a big deletion in *FAH12* sequence, altering its function in castor plant.

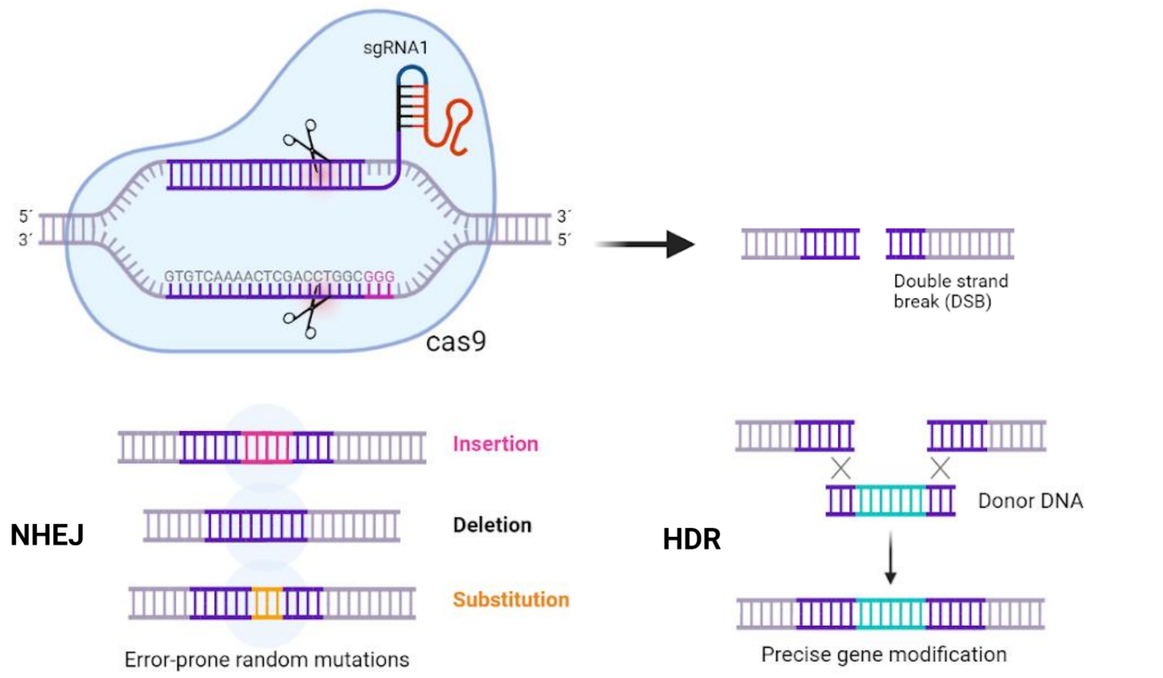

Figure 1. CRISPR/Cas9 gene editing mechanism. cas9 endonuclease is guided by single guide RNA (sgRNA), to a 20-nt DNA sequence (grey) upstream of the protospacer-associated motif (PAM, pink), resulting in double-strand break (DSB) upstream of the NGG. DSBs are therefore repaired by non-homologous end joining (NHEJ) pathway which leads to error-prone random mutations. Alternatively, DSB can be repaired via the error-free homology-directed repair (HDR) pathway using an exogenous donor DNA template for precise gene modification.

GENETIC DESIGN

Two targets with good CRISPR/Cas9 specificity and activity scores were chosen (figure 2). Their 70 pb spacing increases the probability of altering *FAH12*, since repairing the two nearby cuts by NHEJ can result in a large deletion.

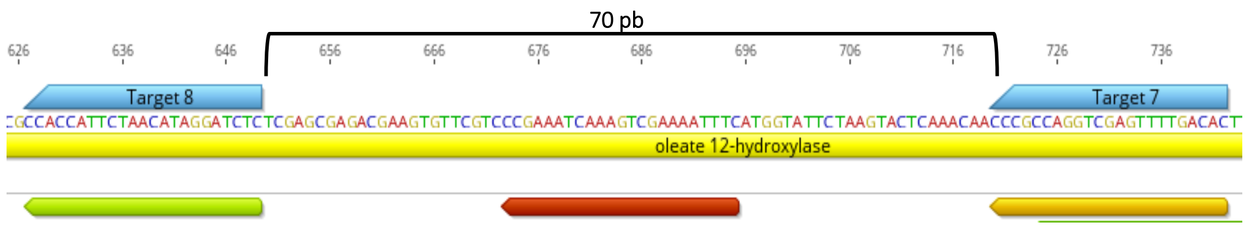

Figure 2. Geneious® software allows us to identify targets in the *FAH12* hydroxylase gene (GenBank U22378) according to the selected requirements. Activity score from (Doench et al., 2016) was used, while specificity score and possible off-targets were detected using castor bean genome as a database.

Level 0. These targets were included in sgRNAs and cloned in level 0 plasmids, each one flanked by restriction sites for *Bsa*I enzyme.

Level 1. Golden Gate level 1 (L1) reaction includes several *Bsa*I digestion and ligation cycles that assemble U6 promoter with both sgRNAs separately into L1 plasmids (B and C in figure 3) flanked by *Bbs*I restriction sites. Simultaneously, cas9 sequence was cloned under the control of a 2x35S promoter followed by the nopaline synthase terminator (nosT) in a similar L1 reaction (A in figure 3).

Level 2. Digestion with *Bbs*I then show compatible overhangs in all of L1 elements (U6-sgRNA1, U6-sgRNA2, 2x35S-Cas9-nosT), which can be assembled in correct order and orientation into a level 2 structure (F, figures 3 and 4). The final result was a level 2 (L2) plasmid including all the elements required for CRISPR/Cas9 multiplex genome editing of *FAH12*, suitable for *Agrobacterium*-mediated stable castor embryos transformation.

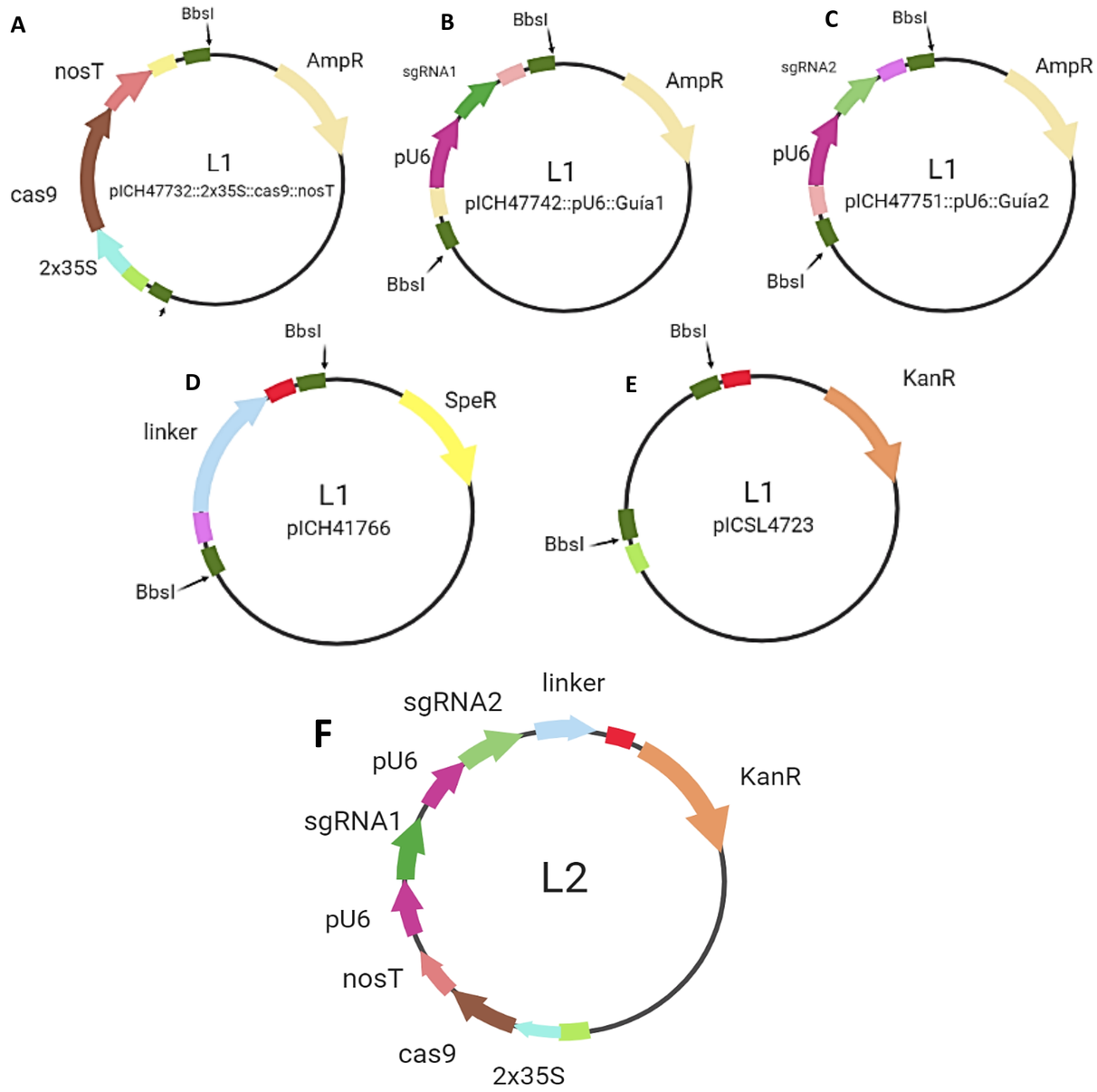

Figure 3. Cloning constructs designed and generated in level 0 to assemble two sgRNAs together with cas9. In the upper part, L1 plasmids (A-F) with *Bbs*I sites and compatible overhangs (coloured squares). They include cas9 (A), both sgRNAs (B and C), a linker sequence (D) and a destination vector (E). These combine together through several *Bbs*I and ligation steps to generate final L2 construct (F), which shows first (green) and final (red) overhangs and include all the elements in correct order and orientation.

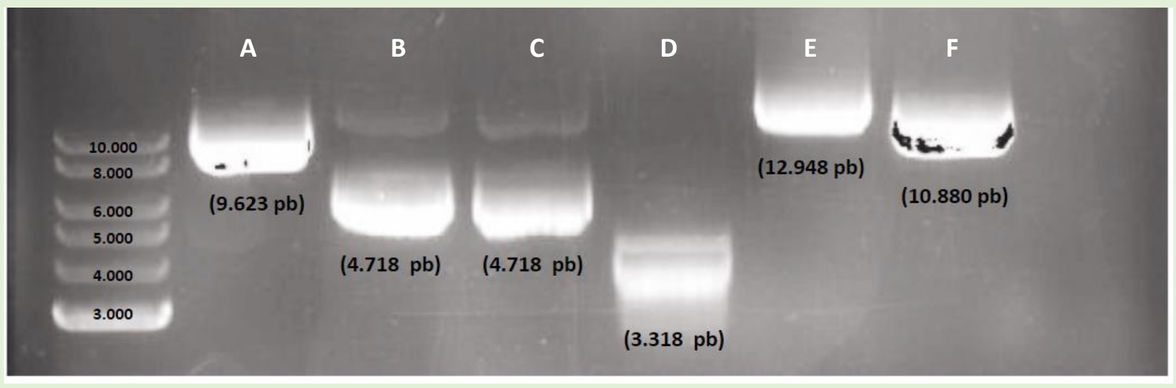

Figure 4. Gel electrophoresis showing all the elements separately assembled: 2x35S-cas9-nosT plasmid (A, 9.623 pb), pU6-sgRNA1 (B, 4.718 pb), pU6-sgRNA2 (C, 4.718 pb), linker (D, 3.318 pb), destination vector (E, 12.948 pb) and final plasmid containing all the elements (F, 10.880 pb).

REFERENCES

Doench, J. G., Fusi, N., Sullender, M., Hegde, M., Vaimberg, E. W., Donovan, K. F., Smith, I., Tothova, Z., Wilen, C., Orchard, R., Virgin, H. W., Listgarten, J., & Root, D. E. (2016). *Nature Biotechnology*, 34(2), pp. 184–191. doi: 10.1038/nbt.3437

Engler, C., Youles, M., Gruetzner, R., Ehnert, T. M., Werner, S., Jones, J. D. G., Patron, N. J. and Marillonnet, S. (2014) *ACS Synthetic Biology*, 3(11), pp. 839–843. doi:10.1021/sb4001504.

Ma, S., Chang, J., Wang, X., Liu, Y., Zhang, J., Lu, W., Gao, J., Shi, R., Zhao, P. and Xia, Q. (2014). *Scientific Reports*, 4, pp. 1–6. doi:10.1038/srep04489.

Sánchez Álvarez, A. J. (2019) "Biotecnología aplicada al ricino para su uso como biofactoría", (Tesis Doctoral).

Shanklin, J., & Cahoon, E. B. (1998). *Annual Review of Plant Biology*, 49, pp. 611–641. doi: 10.1146/annurev.arplant.49.1.611

Venegas-Calerón, M., Sánchez, R., Salas, J. J., Garcés, R. and Martínez-Force, E. (2016). *Planta*, 244(1), pp. 245–258. doi:10.1007/s00425-016-2508-4.

Este trabajo fue financiado por la Secretaría General de Universidades, Investigación y Tecnología del Sistema Andaluz del Conocimiento, dentro del Plan Andaluz de Investigación, Desarrollo e Innovación (PAIDI, 2020) con el número de expediente P20_00072, financiado con fondos FEDER de la Unión Europea.